Supplemental Document

Optics Letters

Electrically tunable metasurface for dual-band spatial light modulation using the epsilon-near-zero effect: supplement

TANMAY BHOWMIK* **AND DEBABRATA SIKDAR**

Department of Electronics and Electrical Engineering, Indian Institute of Technology Guwahati, Guwahati, Assam 781039, India
**Corresponding author:* *tanmay18@iitg.ac.in*

Supplement DOI: https://doi.org/10.6084/m9.figshare.20737021

Parent Article DOI: https://doi.org/10.1364/OL.471974

Electrically-tunable metasurface for dual-band spatial light modulation using epsilon-near-zero effect: Supplemental document

Section-I: Modelling of charge accumulation layer as graded-index layer

The formation of a metal-oxide-semiconductor (MOS) type structure containing Au–Al_2O_3–ITO layers is illustrated in the Fig. S1(a). To study the accumulation of free-carriers upon applying bias voltage, we have conducted electrostatic device simulation in Lumerical Device tool. The voltage-dependent carrier concentration distributions can be seen in Fig. 2(a) for the "first 10 nm from ITO–Al_2O_3 interface" inside the ITO-layer. We have considered the ultra-thin **ac**cumulation **l**ayer (ACL) at the ITO-alumina interface as a 5 nm graded layer, where the change of carrier distributions of each grid (1 nm thick) is calculated from electrostatic solver, as shown in Figs. S1(b) and S1(c).

Following the device physics simulations, the spatial carrier distributions inside the active ACL are translated to the spatial distributions of permittivity via Drude model for consideration in the optical simulations done with Lumerical FDTD tool. This multi-layer (or graded-index layer) approach is more realistic than the conventional two-layer model as mentioned in [1], where an excellent match with experimental results was reported. Note that, the electron mobility (μ) of ACL is 13 $cm^2V^{-1}s^{-1}$, which is lower than the bulk ITO layer having $\mu \approx 19.5$ $cm^2V^{-1}s^{-1}$[2].

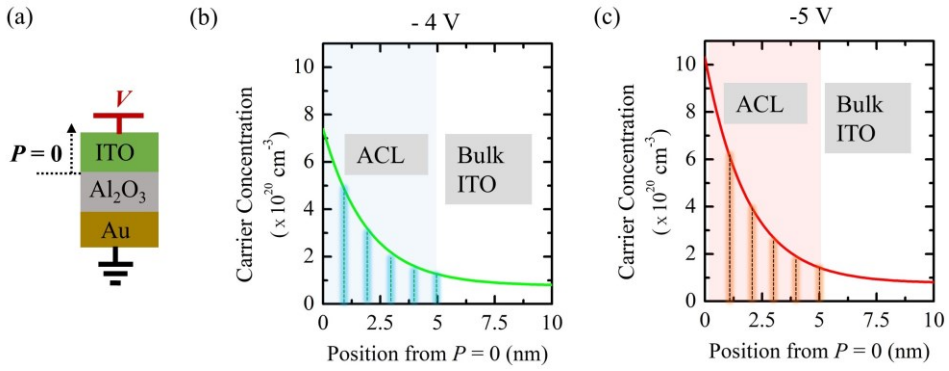

Fig. S1. (a) The formation of MOS-type structure containing Au–Al_2O_3–ITO layers, where P = 0 represents the ITO–Al_2O_3 interface. The variation in carrier concentration distribution, N (cm^{-3}), of ITO layer at the position from P = 0 to 10 nm for (b) –4 V and (c) –5 V bias voltages. Note that the ultra-thin **ac**cumulation **l**ayer (ACL) is considered as a 5 nm graded layer from the ITO–Al_2O_3 interface (highlighted in blue background for –4 V and red background for –5 V).

Section-II: Effective medium theory (EMT)

Effective medium theory (EMT) combined with modal analysis is adopted to observe the guided-mode resonance response. As the grating period of our structure is comparable to operating wavelength region, *i.e.,* $\lambda > \Lambda$ (where λ and Λ are the free-space wavelength of incident light and the grating period, respectively), the second-order expression for EMT, as

mentioned in [3], [4], is considered here. The Si_3N_4 nanograting is modelled as an effective medium with uniform permittivity, given as[3], [4]:

$$\varepsilon_{\text{eff},\parallel}{}^{(2)} = \varepsilon_{0,\parallel} + \frac{\pi^2}{3} f^2(1-f)^2 \times \left(\frac{1}{\varepsilon_s} - \frac{1}{\varepsilon_{\text{Air}}}\right)^2 \varepsilon_{0,\parallel}^3 \, \varepsilon_{0,\perp} \left(\frac{\Lambda}{\lambda}\right)^2 \quad \text{(S1)}$$

where $\varepsilon_{\text{eff},\parallel}{}^{(2)}$ denotes the second-order effective permittivity of nanograting for parallel or x-polarized light. Whereas, the $\varepsilon_{0,\parallel}$ and $\varepsilon_{0,\perp}$ are the zero-order effective permittivity for x- and y-polarized light, respectively, given by [5]:

$$\varepsilon_{0,\parallel} = f(\varepsilon_s) + (1-f)\varepsilon_{\text{Air}} \quad \text{(S2)}$$

$$\varepsilon_{0,\perp} = \varepsilon_s \varepsilon_{\text{Air}} / [f(\varepsilon_{\text{Air}}) + (1-f)\varepsilon_s] \quad \text{(S3)}$$

where ε_s and ε_{Air} are the permittivity of silicon-nitride and air, respectively, and λ is the free-space wavelength.

The filling fraction (*f*) is calculated as $f = \frac{w^2}{\Lambda^2} = 0.75$ for grating period (Λ) and width (w) of 800 nm and 600 nm, respectively.

Section-III: requirement of minimum number of grating periods

The lateral dimensions of the device, or more specifically, the minimum number (P_N) of grating periods required to sustain a sharp guided-mode resonance depends on the Q-factor of the resonance, which can be given by [6]:

$$P_N > Q/\pi\,, \qquad \text{where, } Q = \frac{\Delta\lambda}{\lambda_0}\,, \quad \text{(S4)}$$

where λ_0 is the free-space wavelength of incident light and $\Delta\lambda$ is the spectral bandwidth, which can be expressed by [6]:

$$\Delta\lambda = \frac{\lambda_0 \Lambda}{\pi L}, \quad \text{(S5)}$$

where Λ is the grating period and L is the propagation length (or loss length) of the particular guided-mode, which can be expressed by [7]:

$$L = \frac{\lambda_0}{2\pi \times \Im m(n_{TM})}\,, \quad \text{(S6)}$$

where $\Im m(n_{\text{TM}})$ is the imaginary part of modal index at the resonant wavelength λ_0. Without applying any bias-voltage, we find that normally incident x-polarized plane wave can excite TM_1-mode and TM_2-mode with effective index of (1.932 + 0.01732713i) and (1.629 + 0.008573i), respectively. Thus, the loss length of the TM_1-mode can be calculated as ~15 μm, which results in a spectral bandwidth $\Delta\lambda \approx 26$ nm. Thus, the Q-factor of the resonance for TM_1-mode is 59—leading to $P_N = 19$. On the other hand, with a higher Q-factor of 96 for TM_2-mode, the minimum number (P_N) of grating periods required to sustain a sharp resonance is around 30. So, for our dual-mode design we require at least 30 periods.

Therefore, to accommodate 30 periods of the grating with 800 nm periodicity we need to have a device dimension of around 25 × 25 μm^2 to sustain sharp resonances for both TM_1-mode and TM_2-mode at the vicinity of 1.55 μm and 1.31 μm, respectively.

Section-IV: Modulation speed and frequency-response of the device

To estimate the *RC*-limited electrical bandwidth of the modulator, while maintaining minimum number of grating periods required to sustain a sharp GMR-effect, we need to find the effective device resistance (R) and capacitance (C). The capacitance per unit cell area is estimated as ~10.97 fF/μm^2 by performing electrostatic simulations on Lumerical Device. Thus, for a device dimensions of 25 × 25 μm^2, the total capacitance (C) is approximated as ~6.8 pF.

The effective resistance of the device can be approximated as $R = (R_{ITO} + R_{Gold})/2$, where R_{Gold} is the resistance for the gold layer and R_{ITO} is the resistance for the ITO layer [2]. The value of R_{ITO} can be estimated as the parallel combination of R_{ITO} (for bulk ITO-layer) and R_{ACL} (for charge-accumulation layer) with a carrier concentration, N, of 7×10^{19} cm^{-3} and 6.46×10^{20} cm^{-3}, respectively.

Then, for each corresponding layer, the resistance can be derived by using $R_0 = (\rho l_0/tw_0)$, where w_0 and l_0 are the width and length of the device, respectively. Here, t is the thickness and ρ is the resistivity of the corresponding layer. The resistivity of gold layer can be approximated as 2.2×10^{-8} Ω.m [8]. In contrast, the resistivity of a semiconductor depends on the carrier mobility (μ), given by, $\rho = (e\mu N)^{-1}$.

Thus, the resistivity of bulk ITO-layer (with μ = 19.5 cm^{2}V^{-1}s^{-1}) and accumulation layer (with μ = 13 cm^{2}V^{-1}s^{-1}) can be calculated as 4.57×10^{-5} Ω.m and 7.5×10^{-6} Ω.m, respectively [1]. This results in an effective device resistance (R) of ~280 Ω—leading to a 3-dB bandwidth, $f_{3dB} = (2\pi RC)^{-1}$, of ~83.5 MHz. We can also estimate the bit-rate (BR) of ~167 Mbps by applying Nyquist theorem ($BR = 2 \times f_{3dB} \times \log_2 \kappa$, where $\kappa = 2$ denotes the number of signal levels).

Section-V: Comparative Overview

Table S1. Comparative Overview of a Few Recently Reported ENZ-material Based Modulators

Ref.	λ (μm)	MD (dB)	Speed (Mbps)	Multi-band Operation
Forouzmand *et al.* [9]	1.537	~12.5	NA	No
Kim *et al.* [10]	1.480	~13.3	NA	No
Vatani *et al*. [2]	1.550	24	~80	No
Forouzmand *et al.* [11]	1.547, 1.564	23.3, 23.7	NA	No
Qiu *et al.* [12]	1.510, 1.512	14, 20	NA	No
This Work	1.550, 1.310	**~22.3, ~19.5**	**~167**	**Yes**

Here, MD: modulation depth, λ: operational wavelength, and NA: not available.

A comparative overview with a few recently reported ENZ-material based optical modulators can be seen in Table 1. Here, we would like to emphasize on the fact that most of the previously reported designs are either operated in a single wavelength or dual-wavelengths restricted to a single band. In contrast, our proposed design can operate in both C-band and O-band of wavelength region while maintaining a *MD* as high as ~22.3 dB (at 1.55 μm) and ~19.5 dB (at 1.31 μm), respectively.

Section-VI: Reflectance spectra with silica substrate

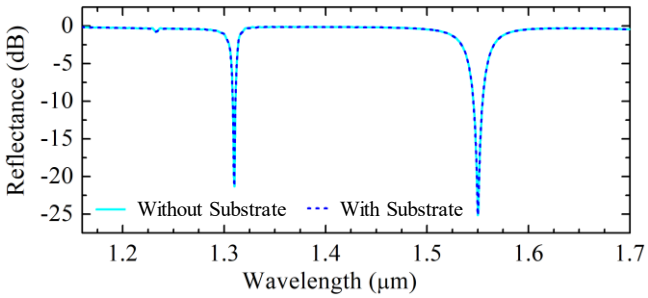

Fig. S2 Reflectance (*R*) spectra, in dB, of the proposed metasurface with a 500 nm thick silica substrate at 0 V bias. The resonance responses occur at 1.55 μm and 1.31 μm for TM_1-mode and TM_2-mode, respectively.

The numerical simulation results reveal that due to the presence of an optically thick Au back-plane, there will be no effect on the resonance dips in the reflectance spectra if we include a 500 nm thick silica substrate, as shown in Fig. S2. Inclusion of a substrate will provide mechanical strength of the device without effecting the resonance dips in the reflection spectra.

References

[1] X. Liu *et al.*, "Tuning of Plasmons in Transparent Conductive Oxides by Carrier Accumulation," *ACS Photonics*, vol. 5, no. 4, pp. 1493–1498, Apr. 2018, doi: 10.1021/acsphotonics.7b01517.

[2] S. Vatani, H. Taleb, and M. K. Moravvej-Farshi, "Optical Modulation via Guided-Mode Resonance in an ITO-Loaded Distributed Bragg Reflector Topped with a Two-Dimensional Grating," *IEEE J. Sel. Top. Quantum Electron.*, vol. 27, no. 3, May 2021, doi: 10.1109/JSTQE.2021.3055736.

[3] D. Wang, Q. Wang, and J. Gao, "Spectral Correlation between 2D and 1D Guided Mode Resonant Filters," *IEEE Photonics Technol. Lett.*, vol. 31, no. 15, pp. 1289–1292, Aug. 2019, doi: 10.1109/LPT.2019.2925770.

[4] Z. Wang, T. Sang, L. Wang, J. Zhu, Y. Wu, and L. Chen, "Guided-mode resonance Brewster filters with multiple channels," *Appl. Phys. Lett.*, vol. 88, no. 25, p. 251115, Jun. 2006, doi: 10.1063/1.2215610.

[5] T. Bhowmik, A. K. Chowdhary, and D. Sikdar, "Grating-Assisted Polarization-Insensitive Dual-Mode Spatial Light Modulator Design Using Epsilon-Near-Zero Material," *IEEE J. Quantum Electron.*, vol. 58, no. 4, pp. 1–8, Aug. 2022, doi: 10.1109/JQE.2022.3166653.

[6] F. Gambino, M. Giaquinto, A. Ricciardi, and A. Cusano, "(INVITED)A review on dielectric resonant gratings: Mitigation of finite size and Gaussian beam size effects," *Results Opt.*, vol. 6, p. 100210, Jan. 2022, doi: 10.1016/J.RIO.2021.100210.

[7] X. Hu, Q. Chen, L. Wen, L. Jin, H. Wang, and W. Liu, "Modulating spatial light by grating slot waveguides with transparent conducting oxides," *IEEE Photonics Technol. Lett.*, vol. 28, no. 15, pp. 1665–1668, Aug. 2016, doi: 10.1109/LPT.2016.2565507.

[8] D. R. Lide, *CRC Handbook of Chemistry and Physics*, 75th ed. New York: CRC Press, 1997.

[9] A. Forouzmand and H. Mosallaei, "Electro-optical Amplitude and Phase Modulators Based on Tunable Guided-Mode Resonance Effect," *ACS Photonics*, vol. 6, no. 11, Nov. 2019, doi: 10.1021/acsphotonics.9b00950.

[10] M. L. Brongersma and S. J. Kim, "Active flat optics using a guided mode resonance," *Opt. Lett. Vol. 42, Issue 1, pp. 5-8*, vol. 42, no. 1, pp. 5–8, Jan. 2017, doi: 10.1364/OL.42.000005.

[11] A. Forouzmand and H. Mosallaei, "Tunable dual-band amplitude modulation with a double epsilon-near-zero metasurface," *J. Opt.*, vol. 22, no. 9, p. 094001, Jul. 2020, doi: 10.1088/2040-8986/ABA03E.

[12] X. Qiu, J. Shi, Y. Li, and F. Zhang, "All-dielectric multifunctional transmittance-tunable metasurfaces based on guided-mode resonance and ENZ effect," *Nanotechnology*, vol. 32, no. 6, p. 065202, Nov. 2020, doi: 10.1088/1361-6528/abc3e5.